ACS OMEGA

Article

Cite This: ACS Omega 2018, 3, 1322−1328

# Wafer-Scale Thermophoretic Dry Deposition of Single-Walled Carbon Nanotube Thin Films

Patrik Laiho,* Mahdi Rafiee, Yongping Liao, Aqeel Hussain, Er-Xiong Ding, and Esko I. Kauppinen*

Department of Applied Physics, Aalto University School of Science, P.O. Box 15100, FI-00076 Aalto, Finland

Supporting Information

**ABSTRACT:** We report the direct and dry deposition of transparent conducting films (TCFs) of aerosol-synthesized single-walled carbon nanotubes (SWNTs) using a thermophoretic precipitator (TP) designed for the uniform and efficient deposition of aerosol-synthesized nanomaterials on 50 mm wafers or similarly sized polymer substrates. The optical and electrical performance of the fabricated TCFs match or surpass the published results achieved using a filter-based collection of aerosol-synthesized SWNTs, and TCFs with sheet resistances of 60 Ω/sq. at 87.8% transmittance and 199 Ω/sq. at 96% transmittance on flexible polymer substrates are demonstrated. The precipitator design is immediately applicable in roll-to-roll fabrication of SWNT TCFs or other functional coatings of aerosol-synthesized nanomaterials.

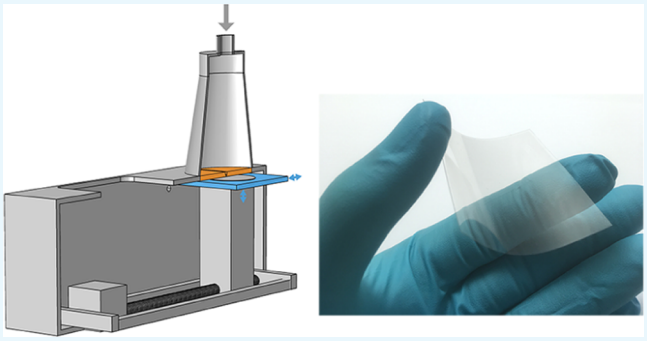

## INTRODUCTION

Thin films of single-walled carbon nanotubes (SWNTs) are an appealing material for transparent conducting films (TCFs) due to their conductivity, flexibility, and low refractive index, with the potential applications in, e.g., touch displays and photovoltaics.[1] As a particular advantage and in contrast to conventional TCF materials such as doped metal oxides, the mechanically robust structure of SWNT-based TCFs makes them applicable in flexible and stretchable electronics.[2] Although SWNT TCFs can be prepared from liquid dispersions of SWNTs by a wide range of coating and printing methods, surfactant contamination and structural damage to the SWNTs caused by dispersion steps limit their performance and applicability. High-performance SWNT TCFs[3] have been previously fabricated by a dry, dispersion-free technique based on collecting the SWNTs, grown in the gas phase using a floating catalyst chemical vapor deposition (FC-CVD) process, on a membrane filter and transferring the SWNT thin film formed on the filter on a target substrate by simply pressing the filter on it.[4] However, the applicability of this method is limited by the availability and cost of suitable filters, it can only be used when the adhesion of the SWNTs on the substrate is stronger than that on the filter membrane, and it requires that the film is thick and forms a continuous, interlinked structure. In addition to filtration, aerosol-synthesized nanomaterials such as FC-CVD SWNTs can be also efficiently deposited using electric fields or temperature gradients in electrostatic[5] or thermophoretic[6] precipitators (ESP, TP), both of which are widely utilized in aerosol sampling. The usefulness of ESPs for the deposition of thin films and coatings, such as SWNT TCFs, is limited by the low charging efficiency of nanoparticles,[7] charging in SWNT aerosols may be increased by gas-phase bundling,[8,9] detrimental to TCF performance,[10] and the uniformity and morphology of SWNTs deposited using ESPs are typically nonideal.[11,12] Conversely, sampling by thermophoresis has the advantage that the deposition rate of nanoscale aerosol particles is generally assumed to be independent of the particle size and morphology, although relatively high-temperature gradients are required to achieve a high deposition efficiency. Because the diameters of engineered nanoparticles $d_p$ are typically close to or smaller than the mean free path of the surrounding gas molecules, the engineering analysis of TPs is commonly based on the free molecular regime model of Waldmann.[13] Briefly, when the thermophoretic force exerted on the aerosol particle by a surrounding temperature gradient is balanced with the free-molecular drag force, the result is a $d_p$-independent terminal velocity $v_{th}$ of the form

$$v_{th} = -\frac{3\mu_g \nabla T}{4\left(1 + \frac{\pi\varphi}{8}\right)\rho_g T} \quad (1)$$

where $\mu_g$ is the gas viscosity, $\nabla T$ is the temperature gradient, $\varphi$ is the momentum accommodation factor, typically assumed to be 0.9, $\rho_g$ is the gas density, and $T$ is the particle temperature. It should be noted, however, that the assumptions of a constant momentum accommodation factor and rigid-body collisions in eq 1 may not be valid when the diameter of the particle or SWNT, $d_p$, is on the order of single nanometers. Li and Wang[14] have proposed modified forms for the drag and thermophoretic

Received: November 28, 2017
Accepted: January 22, 2018
Published: January 31, 2018




DOI: 10.1021/acsomega.7b01869
ACS Omega 2018, 3, 1322−1328

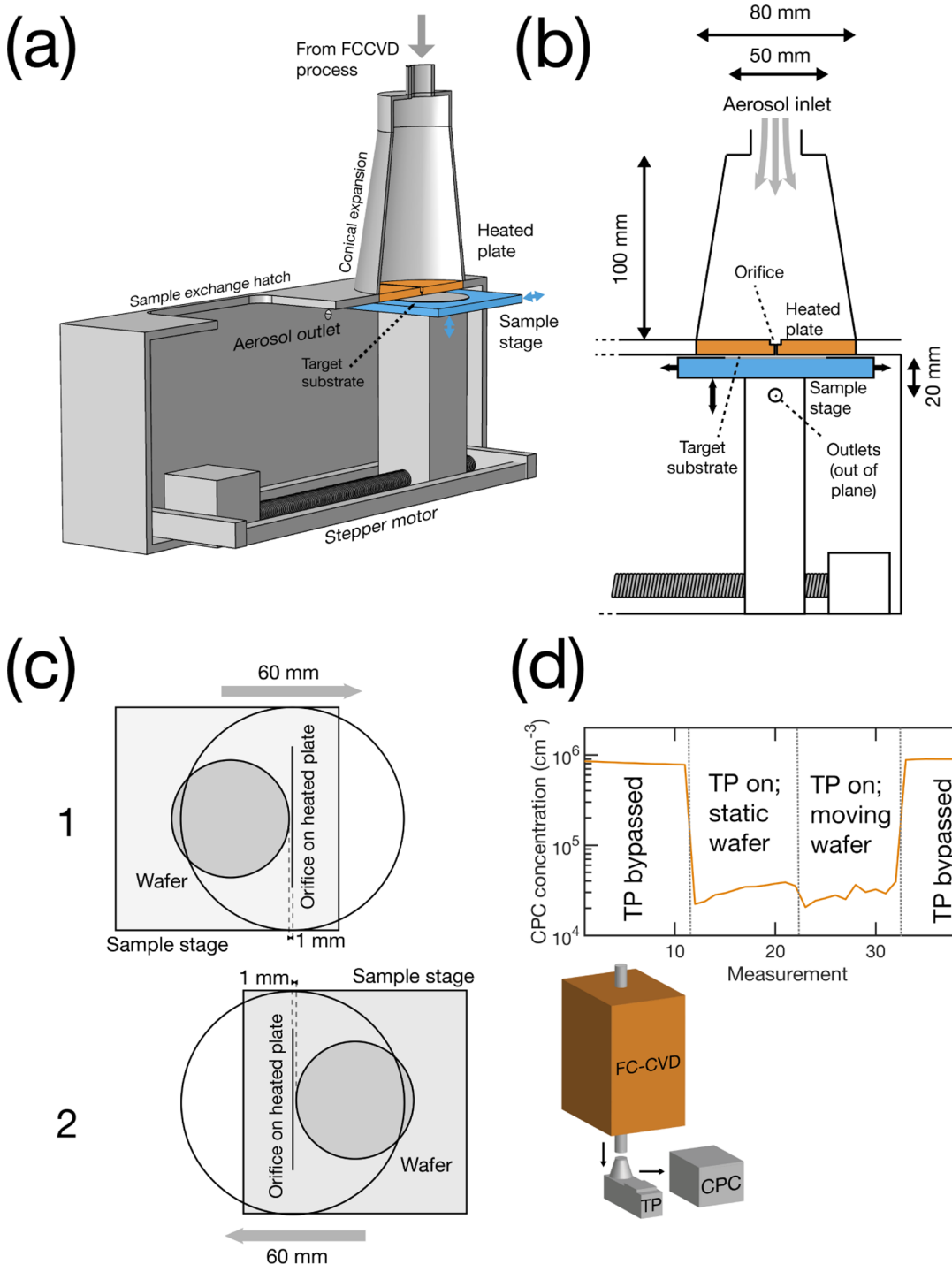


**Figure 1.** Schematics of the TP, the oscillation procedure, and the deposition efficiency. (a) A schematic illustration of the TP design. (b) A profile view of the deposition area, viewed toward the end of the orifice. (c) Oscillation procedure for depositing uniform thin films. The initial distance of the wafer edge and orifice is 1 mm. (d) Deposition efficiency, as measured by CPC. The aerosol number concentration measured through the heated TP, when a temperature gradient of $9.3 \times 10^4$ K/m is applied over a 0.75 mm distance between the hot plate and the substrate, is approximately 2.5% of the concentration measured through a bypass line of similar path length, indicating a high deposition efficiency.

forces, accounting for intermolecular forces between the gas molecules and the particle, and the size dependence of $\varphi$, resulting in

$$v_{th} = \left(1 - \frac{6}{5}\frac{\Omega_{avg}^{(1,2)*}}{\Omega_{avg}^{(1,1)*}}\frac{15\mu_g \nabla T}{4\rho_g T}\right) \quad (2)$$

where the reduced collision integrals $\Omega_{avg}^{(1,2)}$, tabulated in Li and Wang,[14] describe the forces, averaged over diffuse and specular scattering, in the case of the drag ($l = 1$) and the thermophoretic force ($l = 2$). Depending on the temperature and $d_p$, eq 2 may predict a $v_{th}$ even orders of magnitude lower than eq 1. Previously, we have observed[6] that the $v_{th}$s of SWNTs with diameters between 1.2 and 1.9 nm were lower than those predicted by eq 1, and showed a a diameter dependence similar



DOI: 10.1021/acsomega.7b01869
ACS Omega 2018, 3, 1322−1328

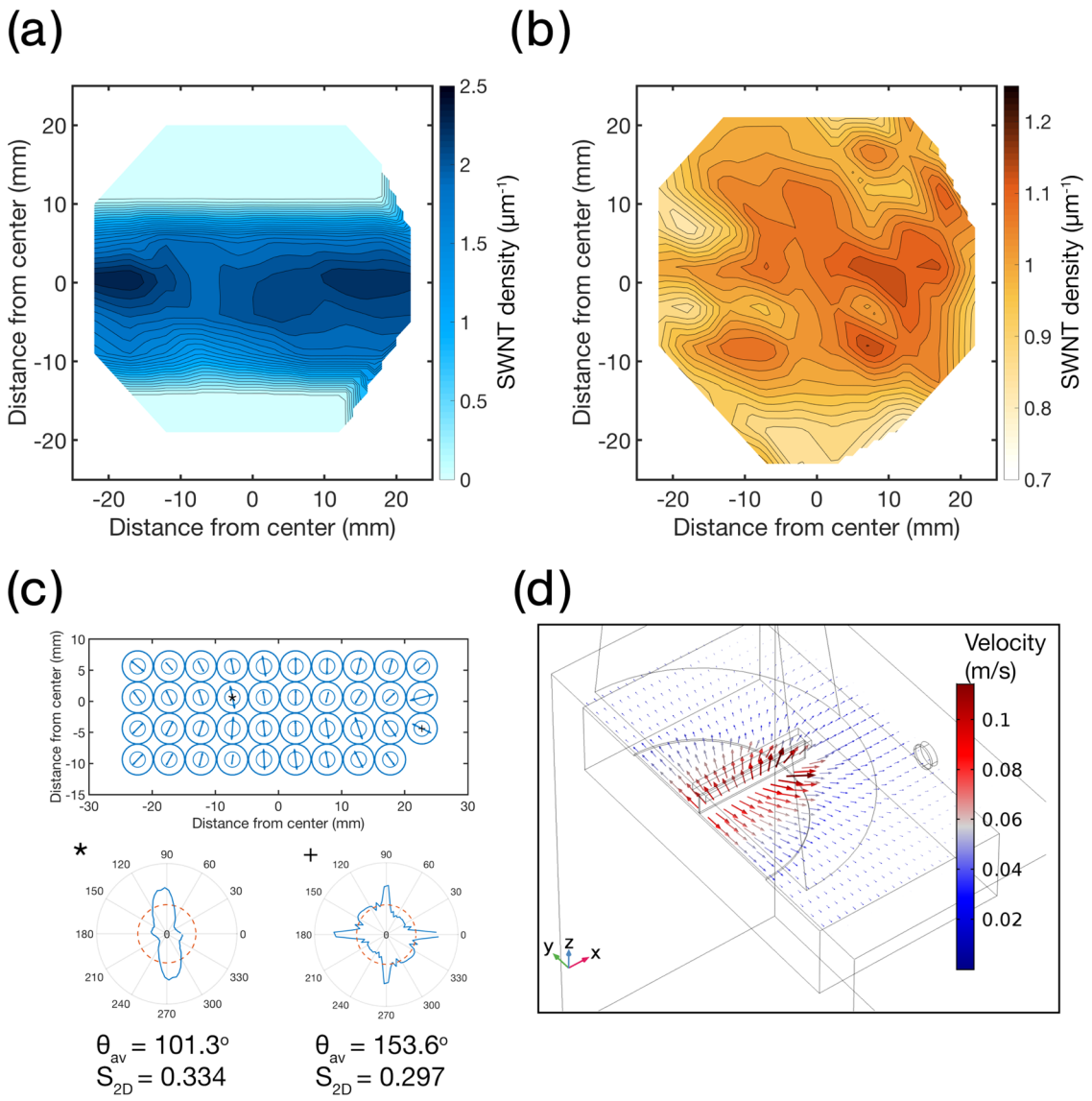


**Figure 2.** Uniformity of the deposited SWNTs and finite-element modeling of the gas flow inside the TP. (a) Normalized SWNT density based on SEM on a 50 mm $Si/SiO_2$ wafer, held stationary under the orifice during deposition. (b) Normalized SWNT density on a $Si/SiO_2$ wafer, oscillated according to Figure 1c. In (a) and (b), the micrographs are obtained with a separation of 5 mm; the contours are interpolations of the density. (c) Orientational distribution of the SWNTs deposited on a static wafer, determined by SEM. The directions of the arrows indicate the mean orientation observed and their lengths indicate the magnitude of $S_{2D}$. The inner and outer circles correspond to the values of $S_{2D}$ = 0.2 and 0.4, respectively. Inset: representative orientation distributions from two micrographs, marked by an asterisk and a cross. The dashed circles corresponds to uniform orientation distributions. (d) Simulated velocity field of the carrier gas in the middle of the 0.75 mm gap between the top of the substrate (a 50 mm wafer) and the hot plate.

to that predicted by eq 2, although the measured values (35−43% of eq 1) were lower than those predicted by eq 2. Similar observations have been reported by Zhang et al.,[15] who deposited titanium oxide nanoparticles with $d_p$ between 6.5 and 14 nm.

TPs have been previously used to evaluate the aerosol size distributions[16] and exposures to nanoscale aerosols,[17,18] and to deposit functional coatings of aerosol-synthesized nanoparticles,[12,19,20] FC-CVD SWNTs[6] and catalyst nanoparticles for supported CVD growth of SWNTs,[21,22] but to date, no reports of SWNT TCFs fabricated using thermophoretic deposition have been published. With the exception of a design by Holunga et al.,[12] capable of uniform deposition on a stationary 150 mm wafer, TPs reported in the literature are typically designed for sampling on microscopy grids or similar small substrates. Here, we present the fabrication of SWNT TCFs based on the direct deposition of FC-CVD SWNTs using a TP designed for the uniform deposition of aerosol-synthesized nanomaterials on 50 mm wafers or polymer substrates of a similar size. The scale of the system is chosen to keep the deposition times reasonable when using a laboratory-scale FC-CVD process for SWNT synthesis, and so the entire surface of the substrate can be imaged using a standard scanning electron microscope (SEM). However, the geometry is readily scalable and can be used in a roll-to-roll process, particularly when used together with a high-yield process or multiple consequential reactors. The design is not specific to the SWNTs synthesized using a FC-CVD process covered here and could be also used to deposit coatings of other aerosol-synthesized functional materials, such as nanoparticles produced using an evaporation−nucleation process,[23] flame synthesis[20] or spark discharge generators,[24] or nanowires grown by aerotaxy.[25]



DOI: 10.1021/acsomega.7b01869
ACS Omega 2018, 3, 1322−1328

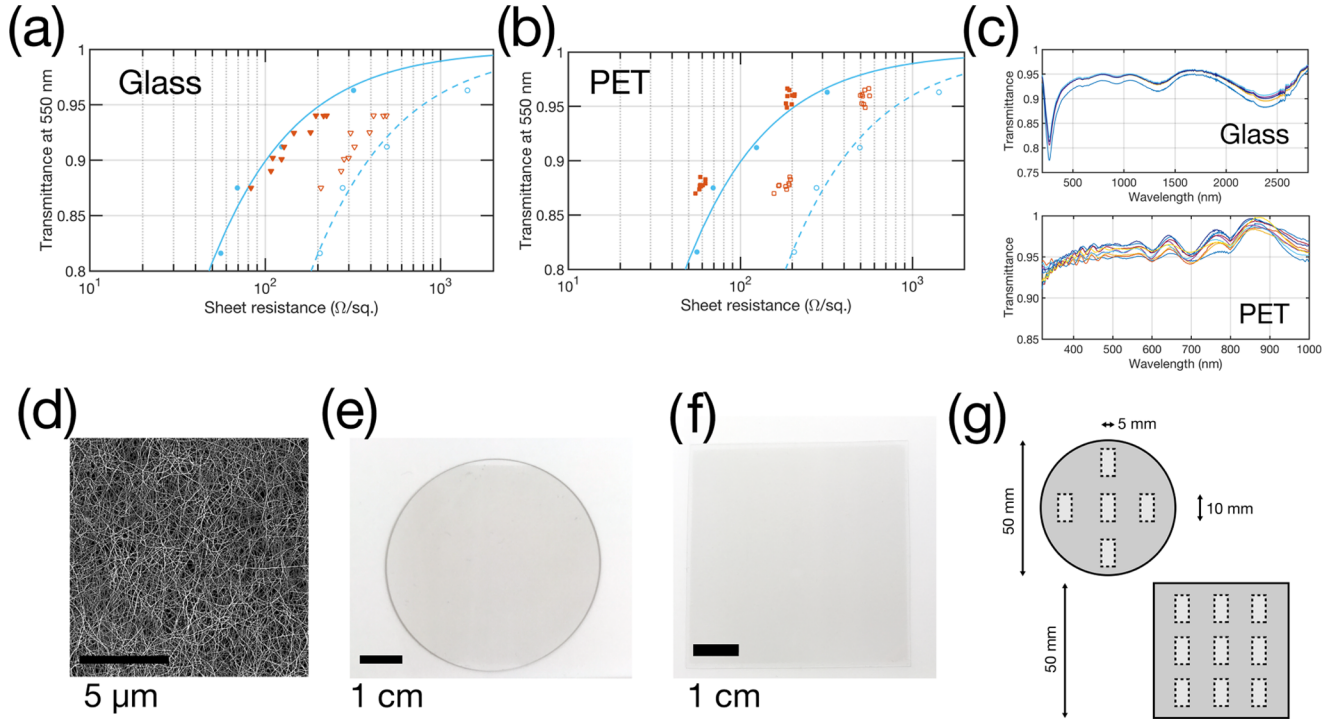


**Figure 3.** SWNT TCFs. (a) Sheet resistance vs transmittance at 550 nm of thermophoretically deposited (red triangles) and press-transferred TCFs (blue circles) on glass. The open symbols indicate pristine and filled symbols indicate doped samples. (b) Sheet resistance vs transmittance at 550 nm of thermophoretically deposited (red squares) and press-transferred (blue circles) TCFs on PET. The open symbols indicate pristine and filled symbols indicate doped samples. In (a) and (b), the blue curves are fits of eq 4 to the press-transferred film data (dashed line indicates pristine, solid line indicates doped samples). (c) Representative transmission spectra from a TCF on glass, recorded at five points and on PET, recorded at nine points. The locations of the measurements are shown in (g). (d) Representative SEM micrograph of a pristine TCF film deposited by TP. (e, f) Photographs of TCFs on a 50 mm borosilicate glass wafer and a 50 mm × 50 mm PET sheet. (g) Locations of the measurements (spectrophotometer spot size: 5 mm × 10 mm) on the wafers and the PET sheets.

## RESULTS AND DISCUSSION

A cut-out graphic and a side profile of the TP designed for the purpose of this work are presented in Figure 1a,b. The aerosol enters through a 25 mm vacuum flange connected to a conical expansion (height 100 mm, top diameter 65 mm, bottom diameter 95 mm) and passes through a rectangular, 60 mm long, and 0.4 mm wide orifice in a hot plate heated using thin-film resistors (Omega Engineering Ltd., U.K.) using a power of 56 W. The target substrate is placed on a water-cooled stage, with lateral dimensions of 100 × 90 $mm^2$. The stage can be moved using stepper motors controlled by a positioning controller (PI GmbH & Co. KG, Germany) in the direction perpendicular to the orifice and vertically to adjust the distance and temperature gradient between the substrate and the hot plate. To increase the uniformity of the deposited film, the sample stage is oscillated under the orifice, as shown in Figure 1c. A stage movement speed of 1.25 mm/s is used in all of the experiments. The carrier gas exits through two 1/4 in. outlets parallel to the ends of the orifice placed symmetrically 20 mm below the top of the lower chamber of the TP. In the experiments described here, the hot plate is heated to a temperature of 90 °C and the sample chuck is held at an ambient temperature of ca. 23 °C using water cooling. The distance between the substrate and the hot plate is kept at 0.75 mm, corresponding to a temperature gradient of approximately 9.3 × $10^4$ K/m in the region between the hot plate and the substrate. For the deposition of SWNTs, the inlet of the TP is connected to the outlet of a FC-CVD reactor, described in detail earlier,[4,26] and a volume flow of 300 $cm^3$/min is sampled from the reactor through the TP using a vacuum line controlled by a needle valve. The high deposition efficiency of the design is confirmed by sampling a condensation particle counter (CPC) with a sample flow of 300 $cm^3$/min to the outlet of the TP and sampling the output of the FC-CVD process alternatively through the heated TP and piece of 1/4″ stainless steel tubing with a similar distance between the inlet and the outlet. The aerosol number concentration sampled through the TP is approximately 2.5% of the concentration sampled through the bypass line, as shown in Figure 1d, indicating a high deposition efficiency.

The spatial uniformity of the deposited SWNTs is evaluated based on the scanning electron microscopy (SEM) of the near-monolayer films deposited on 50 mm $Si/SiO_2$ wafers. When no temperature gradient is applied, few SWNTs (none or a few in a SEM micrograph of 57 $\mu$m × 43 $\mu$m), likely deposited by diffusion, are observed on the wafer. This indicates that SWNTs and particles with smaller aerodynamic diameters will not deposit by inertial impaction in the geometry used here. The observed SWNT density on a wafer kept stationary under the orifice is shown in Figure 2a. SWNTs are observed only on a 20 mm wide region centered on the orifice, with a density inversely proportional to the distance from the orifice. When the wafer is oscillated according to the procedure shown in Figure 1c, a highly uniform coating of SWNTs is observed and the measured SWNT density across the wafer, shown in Figure 2b, is observed to be within 20% of its mean value. We suggest that the main source of the nonuniformity is possibly a slight tilt between the stage and the hot plate, which are difficult to align perfectly in the academic workshop the TP has been built in.



DOI: 10.1021/acsomega.7b01869
ACS Omega 2018, 3, 1322−1328

To guide the design process and to interpret the experimental observations, the flow and temperature fields inside the TP are investigated using computational fluid dynamics and heat transfer simulations. The simulated velocity field between the substrate and the hot plate is shown in Figure 2c. As noted previously by Holunga et al.,[12] heating of the inlet may be necessary at higher volume flow rates to prevent the ambient-temperature carrier gas from disturbing the temperature gradient inside the TP. Based on the simulations, the heat transfer caused by an ambient-temperature inlet volume flow of 300 $cm^3$/min is expected to have a minor effect on the temperature gradient in the design presented here; the results are included as the Supporting Information. The deposited SWNTs are observed to orient themselves with the flow to an extent, similarly to what we have reported in a previous study using a smaller TP.[6] Their orientation distributions are determined using gtFiber, an automatic tool for the analysis of micrographs of fibrous materials,[27] and an example of an analyzed micrograph is included as the Supporting Information. The orientations of the SWNTs deposited on a stationary wafer match the orientation of the simulated velocity field shown in Figure 2c well, indicating that the simulated velocity field is realistic, and that similar modeling can be used to scale the design up to larger substrates or flow rates. The orientation is quantified using the two-dimensional (2D) order parameter

$$S_{2D} = 2\langle \cos^2 \theta_n \rangle - 1 \quad (3)$$

where $\theta_n$ is the angle between an individual fiber pixel and the average orientation of the entire image. On a wafer oscillated under the orifice, the orientation pattern, included as the Supporting Information, is more uniform and the strength of the alignment is smaller, as expected. The alignment of fibrous or rodlike particles such as SWNTs is expected to depend both on the flow velocity and the particle dimensions; this is discussed further in the Supporting Information.

To demonstrate the applicability of the thermophoretically deposited SWNT coating as TCFs, we deposited thin films on 50 mm borosilicate wafers (thickness 500 $\mu$m) and 50 × 50 $mm^2$ poly(ethylene terephthalate) (PET) sheets (thickness 100 $\mu$m). The glass wafers and the PET sheets are attached on the stage by a copper tape, also to mask their edges so that they could be handled without scratching the TCF. The deposited TCFs on a borosilicate glass are hole doped[28] by drop-casting nitric acid ($HNO_3$) on them. Interestingly, $HNO_3$ cannot be used on films deposited on the PET because it cannot wet the SWNT coating and instead, gold(III) chloride[29] in acetonitrile is used. For a comparison with earlier published data, we also collect the films from the same process on nitrocellulose membrane filters and press transferred them on quartz windows and smaller PET sheets. Plots of the TCF performance, expressed in terms of their sheet resistance and optical transmittance at a reference wavelength of 550 nm, are shown in Figure 3a,b. The TCFs fabricated using a press transfer show a performance expected from the synthesis process, with a sheet resistance of approximately 100 Ω/sq. at an optical transmittance of 90%, measured at 550 nm. Previously, Kaskela et al.[4] have used a figure of merit

$$K = -\frac{1}{R_s \ln T} \quad (4)$$

where $R_s$ is the sheet resistance and $T$ is the optical transmittance measured at 550 nm to describe the performance of different SWNT TCFs. Fits of eq 4 on the data measured from the press transferred films are included in Figure 3a,b, to facilitate a comparison of the deposition methods. Pristine TCFs deposited by TP show a slightly higher performance than the press-transferred TCFs on both glass and PET, which can partially result from the measurement procedure: Because a larger number of measurements are carried out per sample, the TCFs deposited by TP are exposed to ambient water and oxygen, which may dope the TCFs to a limited extent, for a longer time. We also expect that when depositing by TP, the deposited pristine SWNT film is more tightly packed because, on the filter, the top layer of the already deposited SWNTs acts as an extension of the filter membrane, preventing the SWNT aerosol from reaching its surface and forming an effectively three-dimensional structure. The local morphology of the SWNTs deposited using both methods is also investigated using atomic force microscopy (AFM) and micrographs and height profile measurements are included as the Supporting Information. After doping, the TCFs deposited using both filtration and the TP show comparable performance on both glass and PET substrates. The limited alignment of the deposited SWNTs does not result in measurable anisotropy in the sheet resistance; details are included in the Supporting Information. UV−vis−NIR absorption spectra of the thermophoretically deposited TCFs on borosilicate glass and visible absorption spectra of TCFs on PET, shown in Figure 3c and measured at the locations indicated by Figure 3g, display the expected spectral features associated with SWNT electronic transitions. The observed variation in the thermophoretically deposited TCF properties on glass show similar variation as the density observed by SEM, and all of the data obtained on the same wafer fit within approximately ±20% of its average when expressed by the reciprocal sheet resistance or absorbance, both of which are expected to depend linearly on the SWNT density. Meanwhile, the observed spatial variation on PET is much lower, approximately ±7%, which could result from the fact that a possible misalignment of the sample stage has a lesser effect on the flow when the substrate is thinner. The obtained TCF performance on PET, with $K$ = 125 $k\Omega^{-1}$, corresponds to a value of ca. 76 Ω/sq. at 90% and is highly competitive with indium-doped tin oxide and other conventional TCF materials on flexible substrates.

## CONCLUSIONS

We have designed a thermophoretic precipitator capable of depositing wafer-scale coatings of aerosol-synthesized nanomaterials, such as SWNTs grown using the FC-CVD process. As a demonstration of a functional coating fabricated using the precipitator, the TCFs deposited from the SWNTs synthesized using a FC-CVD process show a good uniformity and a high performance comparable or superior to previously reported high-performance TCFs fabricated using the same synthesis method and a filter-based transfer process. The method shows particular promise for the TCF deposition on flexible polymer substrates on which SWNT-based TCFs are highly competitive with currently used industrial materials, and it can be also used to deposit SWNTs on mechanically fragile or low−surface energy substrates. The precipitator design presented here is readily scalable for larger substrates or processes with higher flow rates, and can be utilized in a roll-to-roll fabrication process.



DOI: 10.1021/acsomega.7b01869
ACS Omega 2018, 3, 1322−1328

## METHODS

**SWNT Synthesis and Deposition.** The SWNTs were synthesized with a FC-CVD process described in detail earlier, with the difference that here a higher concentration was used to keep the deposition times reasonable on the chosen substrates, and the decreased TCF performance caused by bundling[10,26] was compensated by using a longer reactor (a furnace height of 87 cm and a 105 cm quartz work tube, compared to a furnace height of 55.5 cm and an 85 cm quartz work tube in the system reported previously[26]) and a higher $CO_2$ concentration, yielding the SWNTs with a mean length of 7.6 $\mu$m based on SEM, and a mean diameter of ca. 2.0 nm based on the UV−vis−NIR absorption spectroscopy. The length distribution of the SWNTs and a representative absorption spectrum are included as the Supporting Information. A total flow of 400 $cm^3$/min of carbon monoxide (CO, 99.5%, AGA, Finland) was introduced into a vertical reactor consisting of a quartz work tube (length 1050 mm, external diameter 28 mm, wall thickness 2.2 mm, Finnish Specialglass Oy, Finland) inserted in a furnace (Entech, Sweden) held at a set maximum temperature of 850 °C. A 200 $cm^3$/min flow of CO was introduced to the reactor through a water-cooled injector to create a suitable temperature gradient for ferrocene decomposition and catalyst particle formation at the top of the reactor, a 100 $cm^3$/min flow was mixed with ferrocene and introduced through the water-cooled injector and a 100 $cm^3$/min flow was introduced in the space between the water-cooled injector and the work tube to prevent recirculation at the top of the furnace. Additionally, a 2 $cm^3$/min flow of carbon dioxide ($CO_2$, 99.9993%, AGA, Finland) was introduced to increase the mean diameter and length of the grown SWNTs.[30] The SWNTs were collected from the reactor effluent either using the thermophoretic precipitator or nitrocellulose membrane filters (diameter 13 mm, pore size 0.45 $\mu$m, Millipore).

**Aerosol Concentration Measurements.** The number concentration of the FC-CVD process effluent and the deposition efficiency of the TP were determined using a condensation particle counter (model 5414 CPC; cutoff size, $d_{50}$ = 4 nm; GRIMM Aerosol Technik GmbH, Germany).

**Finite-Element Simulations.** Simulations of the gas flow and heat transfer in the TP were carried out with COMSOL Multiphysics 5.3, a commercial partial differential equation solver based on the finite-element method. A depiction of the geometry and mesh used in the simulations are included as the Supporting Information.

**Thin-Film Characterization and Doping.** The sheet resistances of the TCFs were measured using a four-point probe (Jandel Engineering Ltd., U.K., tip radius 250 $\mu$m, tip spacing 1 mm, loading 60 g) connected to a multimeter (HP 3458, Hewlett Packard), and UV−vis−NIR absorption spectra were measured using an Agilent Cary 5000 UV−vis−NIR spectrophotometer (Agilent Technologies, Inc.). The deposited TCFs on the borosilicate glass were hole doped[28] by drop-casting nitric acid ($HNO_3$, 70%, ACS reagent grade) on the film, waiting for 60 s, and washing the film with deionized water. The deposited TCFs on a borosilicate glass were hole doped using a 16 mM solution of gold(III) chloride[29] ($AuCl_3$, ≥99.99%, Sigma-Aldrich) in acetonitrile (99.999%, Sigma-Aldrich). The solution was drop-casted on the film, left in place for 5 min, and washed off with acetonitrile.

**Scanning Electron Microscopy and Atomic Force Microscopy.** Scanning electron microscopy was carried out using a Zeiss SIGMA VP SEM (Carl Zeiss GmbH, Germany), and the density of the SWNTs was determined by analyzing the number of peaks in SEM scanlines, similarly to our earlier published work.[6] Atomic force microscopy was carried out using a Veeco Dimension 5000 AFM operated in intermittent contact (tapping) mode.

## ASSOCIATED CONTENT

### Supporting Information

The Supporting Information is available free of charge on the ACS Publications website at DOI: 10.1021/acsomega.7b01869.

SWNT length distribution, FEM simulations of heat transfer in the TP deposition area, orientation of SWNTs on an oscillated wafer, details of the micrograph analysis, UV−vis−NIR absorption spectra of pristine and doped SWNT TCFs, sheet resistance measurements carried out with different probe orientations, tabulated sheet resistance and optical transmittance measurements, atomic force microscopy of SWNT TCFs prepared by the TP and by press transfer, and further discussion of the SWNT alignment mechanism (PDF)

## AUTHOR INFORMATION


### Corresponding Authors

*E-mail: patrik.laiho@aalto.fi (P.L.).
*E-mail: esko.kauppinen@aalto.fi (E.I.K.).

### ORCID

Patrik Laiho: 0000-0001-8234-1607


### Notes

The authors declare no competing financial interest.

## ACKNOWLEDGMENTS

The authors wish to thank Joel Salminen, Kari Kääriäinen, Axel Toivonen, and Dr. Antti Kaskela for their contributions to the design of the precipitator components. P.L. acknowledges financial support by the Walter Ahlström Foundation. This work made use of the Aalto University Nanomicroscopy Center (Aalto-NMC) premises.

## REFERENCES


(1) Yu, L.; Shearer, C.; Shapter, J. Recent Development of Carbon Nanotube Transparent Conductive Films. *Chem. Rev.* **2016**, *116*, 13413−13453.

(2) Park, S.; Vosguerichian, M.; Bao, Z. A Review of Fabrication and Applications of Carbon Nanotube Film-Based Flexible Electronics. *Nanoscale* **2013**, *5*, 1727−1752.

(3) Zhang, Q.; Wei, N.; Laiho, P.; Kauppinen, E. I. Recent Developments in Single-Walled Carbon Nanotube Thin Films Fabricated by Dry Floating Catalyst Chemical Vapor Deposition. *Top. Curr. Chem.* **2017**, *375*, 90.

(4) Kaskela, A.; Nasibulin, A. G.; Timmermans, M. Y.; Aitchison, B.; Papadimitratos, A.; Tian, Y.; Zhu, Z.; Jiang, H.; Brown, D. P.; Zakhidov, A.; Kauppinen, E. I. Aerosol-Synthesized SWCNT Networks with Tunable Conductivity and Transparency by a Dry Transfer Technique. *Nano Lett.* **2010**, *10*, 4349−4355.

(5) Zavodchikova, M. Y.; Kulmala, T.; Nasibulin, A. G.; Ermolov, V.; Franssila, S.; Grigoras, K.; Kauppinen, E. I. Carbon Nanotube Thin Film Transistors Based on Aerosol Methods. *Nanotechnology* **2009**, *20*, No. 085201.

(6) Laiho, P.; Mustonen, K.; Ohno, Y.; Maruyama, S.; Kauppinen, E. I. Dry and Direct Deposition of Aerosol Synthesized Single-Walled Carbon Nanotubes by Thermophoresis. *ACS Appl. Mater. Interfaces* **2017**, *9*, 20738−20747.




DOI: 10.1021/acsomega.7b01869
*ACS Omega* 2018, 3, 1322−1328

(7) Mädler, L.; Friedlander, S. K. Transport of Nanoparticles in Gases: Overview and Recent Advances. *Aerosol Air Qual. Res.* **2007**, *7*, 304−342.
(8) Gonzalez, D.; Nasibulin, A. G.; Shandakov, S. D.; Jiang, H.; Queipo, P.; Anisimov, A. S.; Tsuneta, T.; Kauppinen, E. I. Spontaneous Charging of Single-Walled Carbon Nanotubes: A Novel Strategy for the Selective Substrate Deposition of Individual Tubes at Ambient Temperature. *Chem. Mater.* **2006**, *18*, 5052−5057.
(9) Nasibulin, A. G.; Shandakov, S. D.; Anisimov, A. S.; Gonzalez, D.; Jiang, H.; Pudas, M.; Queipo, P.; Kauppinen, E. I. Charging of Aerosol Products During Ferrocene Vapor Decomposition in $N_2$ and Co Atmospheres. *J. Phys. Chem. C* **2008**, *112*, 5762−5769.
(10) Mustonen, K.; Laiho, P.; Kaskela, A.; Susi, T.; Nasibulin, A. G.; Kauppinen, E. I. Uncovering the Ultimate Performance of Single-Walled Carbon Nanotube Films as Transparent Conductors. *Appl. Phys. Lett.* **2015**, *107*, No. 143113.
(11) Timmermans, M. Y.; Estrada, D.; Nasibulin, A. G.; Wood, J. D.; Behnam, A.; Sun, D.-m.; Ohno, Y.; Lyding, J. W.; Hassanien, A.; Pop, E.; Kauppinen, E. I. Effect of Carbon Nanotube Network Morphology on Thin Film Transistor Performance. *Nano Res.* **2012**, *5*, 307−319.
(12) Holunga, D. M.; Brunelli, N. A.; Flagan, R. C. A Tool for Uniform Coating of 300-mm Wafers with Nanoparticles. *J. Nanopart. Res.* **2013**, *15*, No. 2027.
(13) Waldmann, L.; Schmitt, K. H. Thermophoresis and Diffusiophoresis of Aerosols. In *Aerosol Science*; Davies, C. N., Ed.; Academic Press Inc.: London, 1966; pp 137−162.
(14) Li, Z.; Wang, H. Thermophoretic Force and Velocity of Nanoparticles in the Free Molecule Regime. *Phys. Rev. E* **2004**, *70*, No. 021205.
(15) Zhang, Y.; Li, S.; Yan, W.; Yao, Q. Nanoparticle Transport and Deposition in Boundary Layer of Stagnation-Point Premixed Flames. *Powder Technol.* **2012**, *227*, 24−34.
(16) Lorenzo, R.; Kaegi, R.; Gehrig, R.; Scherrer, L.; Grobéty, B.; Burtscher, H. A Thermophoretic Precipitator for the Representative Collection of Atmospheric Ultrafine Particles for Microscopic Analysis. *Aerosol Sci. Technol.* **2007**, *41*, 934−943.
(17) Azong-Wara, N.; Asbach, C.; Stahlmecke, B.; Fissan, H.; Kaminski, H.; Plitzko, S.; Bathen, D.; Kuhlbusch, T. A. J. Design and Experimental Evaluation of a New Nanoparticle Thermophoretic Personal Sampler. *J. Nanopart. Res.* **2013**, *15*, No. 1530.
(18) Thayer, D.; Koehler, K. A.; Marchese, A.; Volckens, J. A Personal, Thermophoretic Sampler for Airborne Nanoparticles. *Aerosol Sci. Technol.* **2011**, *45*, 744−750.
(19) Mädler, L.; Roessler, A.; Pratsinis, S. E.; Sahm, T.; Gurlo, A.; Barsan, N.; Weimar, U. Direct Formation of Highly Porous Gas-Sensing Films by in situ Thermophoretic Deposition of Flame-Made Pt/$SnO_2$ Nanoparticles. *Sens. Actuators, B* **2006**, *114*, 283−295.
(20) Teoh, W. Y.; Amal, R.; Mädler, L. Flame Spray Pyrolysis: An Enabling Technology for Nanoparticles Design and Fabrication. *Nanoscale* **2010**, *2*, 1324−1347.
(21) Gonzalez, D.; Nasibulin, A. G.; Baklanov, A. M.; Shandakov, S. D.; Brown, D. P.; Queipo, P.; Kauppinen, E. I. A New Thermophoretic Precipitator for Collection of Nanometer-Sized Aerosol Particles. *Aerosol Sci. Technol.* **2005**, *39*, 1064−1071.
(22) Na, H.; Park, J. H.; Hwang, J.; Kim, J. Site-Specific Growth and Density Control of Carbon Nanotubes by Direct Deposition of Catalytic Nanoparticles Generated by Spark Discharge. *Nanoscale Res. Lett.* **2013**, *8*, No. 409.
(23) Scheibel, H. G.; Porstendörfer, J. Generation of Monodisperse Ag- and NaCl-Aerosols with Particle Diameters between 2 and 300 nm. *J. Aerosol Sci.* **1983**, *14*, 113−126.
(24) Schwyn, S.; Garwin, E.; Schmidt-Ott, A. Aerosol Generation by Spark Discharge. *J. Aerosol Sci.* **1988**, *19*, 639−642.
(25) Heurlin, M.; Magnusson, M. H.; Lindgren, D.; Ek, M.; Wallenberg, L. R.; Deppert, K.; Samuelson, L. Continuous Gas-Phase Synthesis of Nanowires with Tunable Properties. *Nature* **2012**, *492*, 90−94.
(26) Kaskela, A.; Laiho, P.; Fukaya, N.; Mustonen, K.; Susi, T.; Jiang, H.; Houbenov, N.; Ohno, Y.; Kauppinen, E. I. Highly Individual SWCNTs for High Performance Thin Film Electronics. *Carbon* **2016**, *103*, 228−234.
(27) Persson, N. E.; McBride, M. A.; Grover, M. A.; Reichmanis, E. Automated Analysis of Orientational Order in Images of Fibrillar Materials. *Chem. Mater.* **2017**, *29*, 3−14.
(28) Geng, H.-Z.; Kim, K. K.; So, K. P.; Lee, Y. S.; Chang, Y.; Lee, Y. H. Effect of Acid Treatment on Carbon Nanotube-Based Flexible Transparent Conducting Films. *J. Am. Chem. Soc.* **2007**, *129*, 7758−7759.
(29) Kim, K. K.; Bae, J. J.; Park, H. K.; Kim, S. M.; Geng, H.-Z.; Park, K. A.; Shin, H.-J.; Yoon, S.-M.; Benayad, A.; Choi, J.-Y.; Lee, Y. H. Fermi Level Engineering of Single-Walled Carbon Nanotubes by $AuCl_3$ Doping. *J. Am. Chem. Soc.* **2008**, *130*, 12757−12761.
(30) Tian, Y.; Timmermans, M. Y.; Partanen, M.; Nasibulin, A. G.; Jiang, H.; Zhu, Z.; Kauppinen, E. I. Growth of Single-Walled Carbon Nanotubes with Controlled Diameters and Lengths by an Aerosol Method. *Carbon* **2011**, *49*, 4636−4643.


DOI: 10.1021/acsomega.7b01869
*ACS Omega* 2018, 3, 1322−1328